Ab Initio Study of C_4H_3 Potential Energy Surface and Reaction of Ground-State Carbon Atom with Propargyl Radical

TRUNG NGOC LE,[1,2] ALEXANDER M. MEBEL,[2] RALF I. KAISER[1,3,*]

[1]*Institute of Atomic and Molecular Sciences, Academia Sinica, P. O. Box 23-166, Taipei 10764, Taiwan, Republic of China*
[2]*Department of Chemistry, University of Danang, Danang, Vietnam*
[3]*Department of Physics, National Taiwan University, Taipei 106, Taiwan, Republic of China*

Dedicated to Professor Paul von R. Schleyer

ABSTRACT: The potential energy surface for the reaction of the ground-state carbon atom $[C(^3P_j)]$ with the propargyl radical $[HCCCH_2(X^2B_1)]$ is investigated using the G2M(RCC,MP2) method. Numerous local minima and transition states for various isomerization and dissociation pathways of doublet C_4H_3 are studied. The results show that $C(^3P_j)$ attacks the π system of the propargyl radical at the acetylenic carbon atom and yields the n-$C_4H_3(^2A')$ isomer **i3** after an 1,2-H atom shift. This intermediate either splits a hydrogen atom and produces singlet diacetylene, $[HCCCCH$ (**p1**) $+ H]$ or undergoes (to a minor amount) a 1,2-H migration to i-$C_4H_3(^2A')$ **i5**, which in turn dissociates to **p1** plus an H atom. Alternatively, atomic carbon adds to the triple $C\equiv C$ bond of the propargyl radical to form a three-member ring C_4H_3 isomer **i1**, which ring opens to **i3**. Diacetylene is concluded to be a nearly exclusive product of the $C(^3P_j) + HCCCH_2$ reaction. At the internal energy of 10.0 kcal/mol above the reactant level, Rice–Ramsperger–Kassel–Marcus calculations show about 91.7% of HCCCCH comes from fragmentation of **i3** and 8.3% from **i5**. The other possible minor channels are identified as $HCCCC + H_2$ and $C_2H + HCCH$.   © 2001 John Wiley & Sons, Inc.   J Comput Chem 22: 1522–1535, 2001

Introduction

The chemical reaction dynamics of atomic carbon in its C(^{3}P$_j$) electronic ground state with unsaturated hydrocarbon molecules are of major importance in interstellar chemistry,[1, 2] combustion processes,[3] and chemical vapor deposition.[4] Several planets and moons of our solar system are known to have hydrocarbons as significant constituents of their atmospheres.[5] These hydrocarbons are formed from methane through solar radiation and electron bombardment. The atmospheres of Titan, a moon of Saturn,[6, 7] Neptune,[8] Uranus,[9, 10] Triton,[11] Jupiter,[12] and Saturn[13] also have significant methane photochemistry. Analysis of spectra from the Voyager missions led to the unambiguous identification of diacetylene as a constituent of the atmosphere of Titan.[14] As a result, diacetylene is currently one of the most complex hydrocarbons confirmed to be present in planetary atmospheres outside our own.
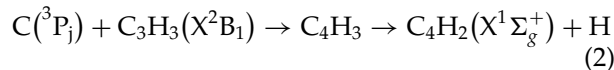
Diacetylene (butadiyne) is the simplest hydrocarbon with conjugated triple bonds and its electronically excited states are thus important testing grounds for theories of electronic structure. The electronic structure of diacetylene was recorded at the various regions of the UV and vacuum UV absorption spectrum.[15–21] Diacetylene plays an important role in the stratospheres of several solar system planets and moons analogous to that played by ozone in Earth's atmosphere.[6] First, C$_4$H$_2$ is known to be photochemically very reactive and hence capable of producing yet larger hydrocarbon molecules[22] such as C$_6$H$_2$ (+ C$_2$H$_2$), C$_8$H$_2$ (+ 2H, H$_2$), and C$_8$H$_3$ (+ H). Second, the large C$_n$H$_2$ polyacetylenes, which are assumed to be the products of diacetylene photochemistry, are proposed as a potential source of the visible absorptions in aerosol hazes present in the planetary atmospheres.[6–13] Third, diacetylene is noteworthy for its role in soot formation, especially in acetylene flames.[23] In addition, diacetylene was also shown to be a significant product in the pyrolytic and photochemical processes involving acetylene.[24, 25] Rate constants for the pyrolytic loss of diacetylene as a function of temperature were also determined,[24] but little is known about the nature of the pyrolysis products or the mechanisms of the pyrolysis reaction.

Despite the importance of diacetylene (C$_4$H$_2$), its synthetic route is far from being characterized satisfactorily. Some reactions were suggested,[26, 27] such as

$$C_2H + C_2H_2 \rightarrow C_4H_2 + H \qquad (1)$$

and

$$C(^3P_j) + C_3H_3(X^2B_1) \rightarrow C_4H_3 \rightarrow C_4H_2(X^1\Sigma_g^+) + H \qquad (2)$$

The rate constants for reaction (1) were measured at temperatures from 295 to 15 K.[28] The results confirmed that C$_2$H radicals reacted rapidly with acetylene at very low temperatures, and the radical replaced a hydrogen atom in C$_2$H$_2$. Reaction (2) was investigated at an average collision energy of 10.0 kcal/mol and the crossed molecular beam technique and a universal mass spectrometric detector were employed.[27]

Recently, we studied various reaction mechanisms of C(^{3}P$_j$) with acetylene (C$_2$H$_2$),[2] ethylene (C$_2$H$_4$),[29] vinyl radical (C$_2$H$_3$),[30] methylacetylene (CH$_3$CCH), allene (H$_2$CCCH$_2$),[31] some other hydrocarbons,[32] and their reaction products by employing *ab initio* calculations and chemical dynamics. Our goal in the present article was to investigate the global potential energy surface (PES) for the doublet C$_4$H$_3$ system. The study provides a deeper, detailed insight into the reaction mechanism, surmises the most significant reaction channels of this important atom–radical reaction, and predicts branching ratios of various products based on Rice–Ramsperger–Kassel–Marcus (RRKM) calculations.

Computational Methods

In the present study we considered geometric configurations of C$_4$H$_3$ and C$_4$H$_2$ relevant to the C(^{3}P$_j$) + C$_3$H$_3$(X^{2}B$_1$) reaction. Most of the topologically possible structures of these species were calculated, although we could not exclude that some other higher energy isomers may exist. The geometries of various isomers of the doublet C$_4$H$_3$ (most of the structures reported here were calculated earlier by us[31] and in the literature[33]), transition states for isomerization and dissociation, as well as the C$_4$H$_2$ dissociation products were optimized using the hybrid density functional B3LYP method[34] with the 6-311G(d,p) basis set.[35] Vibrational frequencies calculated at the same level were used for characterization of stationary points and zero-point energy (ZPE) correction without scaling. All the stationary points were positively identified for a minimum

[number of imaginary frequencies (NIMAG) = 0] or a transition state (NIMAG = 1). When necessary, intrinsic reaction coordinate (IRC) calculations were performed to confirm the identity of a transition state and the two equilibrium structures it connects. All the energies quoted and discussed include the ZPE correction. In some cases mentioned in the Discussion, geometries and frequencies were also calculated at the MP2/6-311G(d,p)[36] level.

In order to obtain more reliable energy [approximation to the RCCSD(T)/6-311+G(3df,2p) energy[37]] for the most important equilibrium structures and transition states, we used the G2M(RCC,MP2) method.[38] The G2-type methods are expected to be accurate to 1–2 kcal/mol based on extensive calculations of various energetic properties for the G2 test set of molecules.[38–41] The G2M(RCC,MP2) scheme is only slightly less accurate than G2M[38] but represents a reasonable compromise between the accuracy and computational demands for the C_4H_3 system. The Gaussian 98[42] program was employed for the calculations.

According to the RRKM theory,[43] the rate constant $k(E)$ at available energy E for a unimolecular reaction $A^* \rightarrow A^\# \rightarrow P$ can be expressed as

$$k(E) = \frac{\sigma}{h} \cdot \frac{W^\#(E - E^\#)}{\rho(E)}$$

where σ is the symmetry factor, $W^\#(E - E^\#)$ denotes the total number of states of the transition state (activated complex) $A^\#$ with the barrier $E^\#$, $\rho(E)$ represents the density of states of the reactant molecule A^*, and P is the product or products. The saddle point method[43] was applied to evaluate $\rho(E)$ and $W(E)$.

Results and Discussion

The optimized structural parameters obtained at the B3LYP/6-311G(d,p) level are displayed in Figures 1 and 2. The graph of possible isomerization and dissociation pathways on the global PES of the C_4H_3 radical is illustrated in Figure 3, and the most important reaction pathways for $C(^3P_j) + C_3H_3(X^2B_1)$ are shown in Figure 4. The intermediates and the dissociation products (C_4H_2) are denoted with the letters **i** and **p**, respectively. The notation tsxy designates a transition state connecting equilibrium structures x and y. The calculated total, zero-point vibrational, and relative energies for all structures obtained at various levels of theory are summarized in Table I. The vibrational frequencies calculated at the B3LYP/6-311G(d,p) level and

Cartesian coordinates of various species are given in the Supplementary Material. Table II compiles RRKM rate constants for different internal energies above the reactant level. Branching ratios for distinct reaction channels are shown in Table III. In this section we present the results of our *ab initio* calculations and feasible reaction pathways on the doublet C_4H_3 PES to produce C_4H_2 isomers plus H and other reaction products.

CARBON ADDITION TO ACETYLENIC CARBON ATOM AND INSERTION INTO C—H BONDS

The *ab initio* calculations revealed that the carbon atom can be added without an entrance barrier to the π system at the propargyl acetylenic carbon atom, yielding a C_4H_3 isomer (**i2**). In principle, two conformations of $CC(H)CCH_2$ are possible, trans and cis, but only the trans structure **i2** was found. **i2** was stabilized by 78.5 kcal/mol with respect to the reactants $C(^3P_j) + HCCCH_2(X^2B_1)$, but it was unstable kinetically. The barrier for an H shift from CH to the terminal carbon atom yielding **i3** was very low, of only 0.1 and 0.3 kcal/mol at the B3LYP and CCSD(T)/6-311G** levels, respectively, and disappeared when ZPE corrections were included. At the G2M(RCC,MP2) level the tsi2i3 was 2.5 kcal/mol below **i2**, indicating that **i2** was most likely not a local minimum. Thus, the reaction was suggested to proceed from $C + HCCCH_2$ to **i3** via carbon addition followed by a barrierless 1,2-H shift.

Despite a careful search we could not find a transition state for carbon atom insertion into C—H bonds of the CH_2 group of the propargyl radical, which would lead to structure **i5**. We started the saddle point optimization from a geometry with a CCH three-member ring suggesting that the C—H bond of propargyl can be concertedly broken with formation of two new bonds C—C and C—H. However, the energies of such structures are high and the optimization did not converge to a transition state. This indicated that the low energy pathway leading from the reactants to **i5** involved formation of **i3** followed by the 1,2-H shift but not an insertion into the C—H bond of the CH_2 group.

CARBON ADDITION TO TRIPLE C≡C BOND

The carbon atom can also attack the triple C≡C bond of the propargyl radical without an entrance barrier and form a doublet cyclopropenylidene (**i1**) with C_s symmetry and the $^2A'$ electronic state, which lies 101.7 kcal/mol below the reactants. Isomer **i1** can isomerize by ring opening to n-C_4H_3 (isomer **i3**), which represents the global
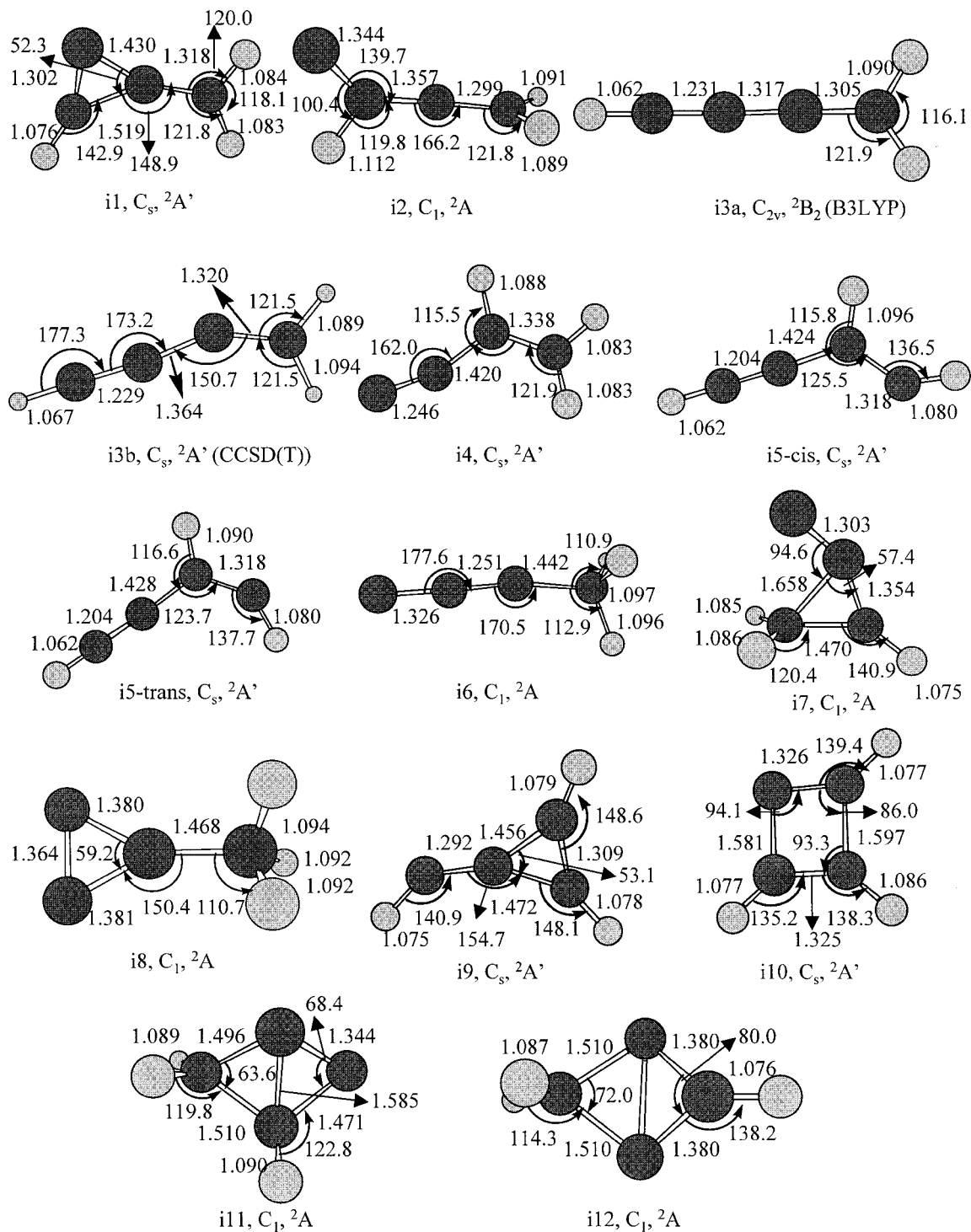
FIGURE 1. The optimized geometries [bond lengths (Å) and bond angles (°)] of various local minima of the C$_4$H$_3$ radical and the possible products. The symmetry point groups and electronic states are also shown.

minimum of the doublet C$_4$H$_3$ PES. Our earlier CCSD(T) calculations[32] showed that in the ground electronic state **i3** has C_s symmetry and the $^2A'$ electronic term. At the G2M(RCC,MP2) level, **i3**

is bound by 131.2 kcal/mol with respect to the C(^3P_j) + C$_3$H$_3$(X$^2B_1$). In addition, **i1** can convert to bicyclic isomers **i12** and **i11** by ring closure through the barriers of 20.0 kcal/mol and 31.7 kcal/mol,
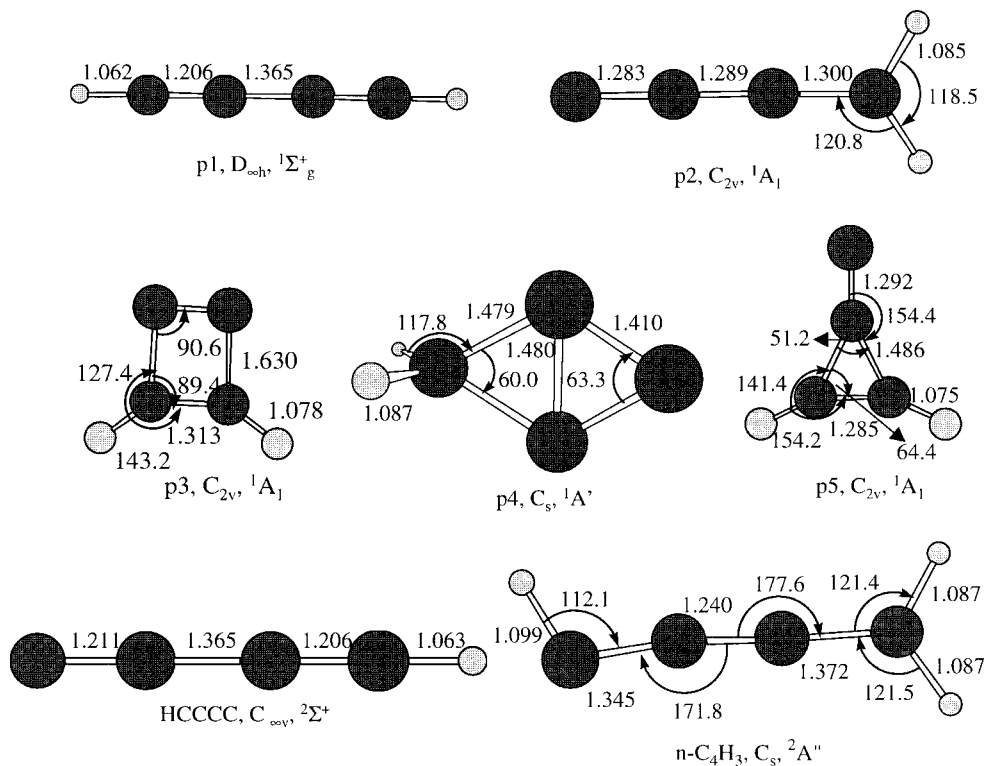
FIGURE 1. (Continued)

while those for the reverse reactions are 19.1 and 12.1 kcal/mol, respectively. Isomer **i11** can undergo a H-atom migration to **i12** with a barrier of 45.1 kcal/mol. At the G2M(RCC,MP2) level, we predicted **i11** and **i12** to be respectively 49.1 and 30.4 kcal/mol higher in energy than **i3**.

We also investigated the addition of the carbon atom to the C of the CH_2 group of C_3H_3 but failed to find any local minimum on the C_4H_3 PES corresponding to this process. Therefore, this addition is not expected to occur in the $C(^3P_j) + C_3H_3(X^2B_1)$ reaction.

OTHER ISOMERIZATION MECHANISMS OF C_4H_3

The n-C_4H_3 isomer **i3** can undergo a 1,2-H shift to i-$C_4H_3(^2A')$ **i5** with a barrier of 53.2 kcal/mol. The latter can also be formed by the ring opening of **i9** (C_s, $^2A'$) and **i10** (C_s, $^2A'$) through the barriers of 6.0 and 15.1 kcal/mol. Isomers **i9** and **i10** lie 31.7 and 47.1 kcal/mol, respectively, higher in energy than **i3**. Isomer **i10** can undergo two successive H-atom migrations to **i11** and **i12** through barriers of 39.5 and 35.1 kcal/mol, respectively. The other isomerization channels of **i3** include a 1,3-H shift to produce **i4** and a 1,4-H migration to form **i6**. However, the barriers for these migrations are fairly high at 82.7 and 91.6 kcal/mol, respectively. Isomer **i4** can

isomerize by ring closure to **i7** (C_1, ^2A) with a barrier of 24.7 kcal/mol, while that for the reverse reaction is only 8.3 kcal/mol. Isomer **i7** lies 50.6 kcal/mol above **i3** and can also be formed by ring opening in **i11** with a barrier of 9.0 kcal/mol. Besides, **i4** can undergo a 1,2-H shift to **i6** with a barrier of 43.1 kcal/mol. The C_4H_3 isomer **i6** has no symmetry and lies 39.5 kcal/mol higher in energy than **i3**. The isomerization of **i6** to **i8** (C_1, ^2A) is hindered by a barrier of 24.5 kcal/mol. Isomer **i8** can be formed from **i11** by a 1,2-H shift accompanied by the cleavage of the C—C bond through a transition state that is 46.6 kcal/mol above **i11**. At the G2M(RCC,MP2) level **i8** lies 34.8 kcal/mol higher in energy than **i3**.

DISSOCIATION PATHWAYS OF C_4H_3

The mechanisms of the C_4H_3 dissociation leading to different singlet C_4H_2 isomers + H and $HCCCC(C_{\infty v}, ^2\Sigma^+) + H_2$ are shown in Figure 3. This study confirmed five different isomers of C_4H_2. The most stable structure was singlet diacetylene (**p1**) with $D_{\infty h}$ symmetry and the $^1\Sigma_g^+$ electronic state, which lies 90.3 kcal/mol below $C(^3P_j) + HCCCH_2(X^2B_1)$. Diacetylene **p1** can be produced by H elimination from **i3** and **i5**. Our calculations gave
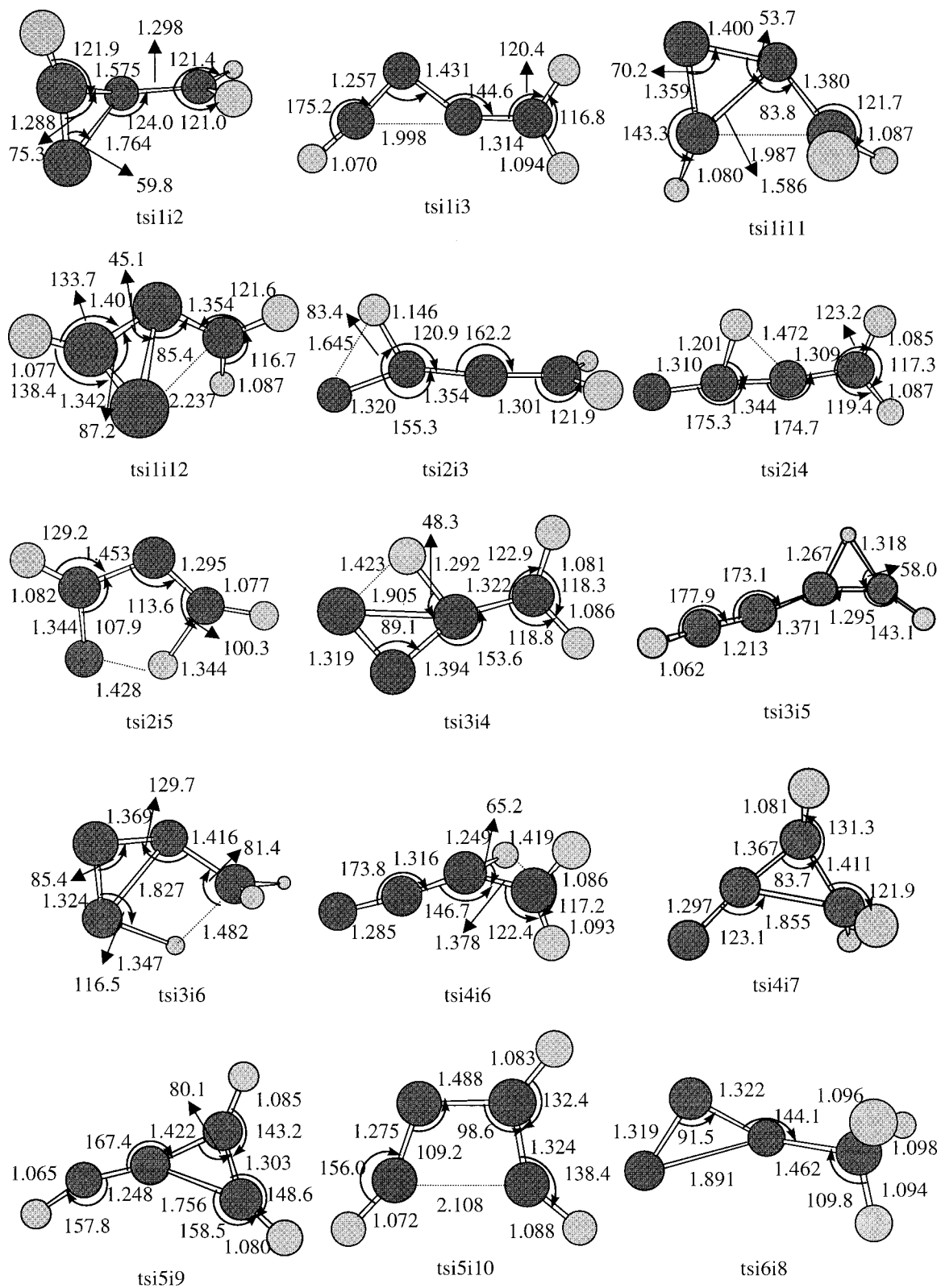
FIGURE 2. The optimized geometries [bond lengths (Å) and bond angles (°)] of various transition states.

FIGURE 2. (Continued)

TABLE I.

Total (hartree), Zero-Points Vibrational and Relative (kcal/mol) Energies of C$_4$H$_3$ and C$_4$H$_2$ Isomers, and Transition States for C$_4$H$_3$ Isomerization and Dissociation as Calculated at Different Levels of Theory.

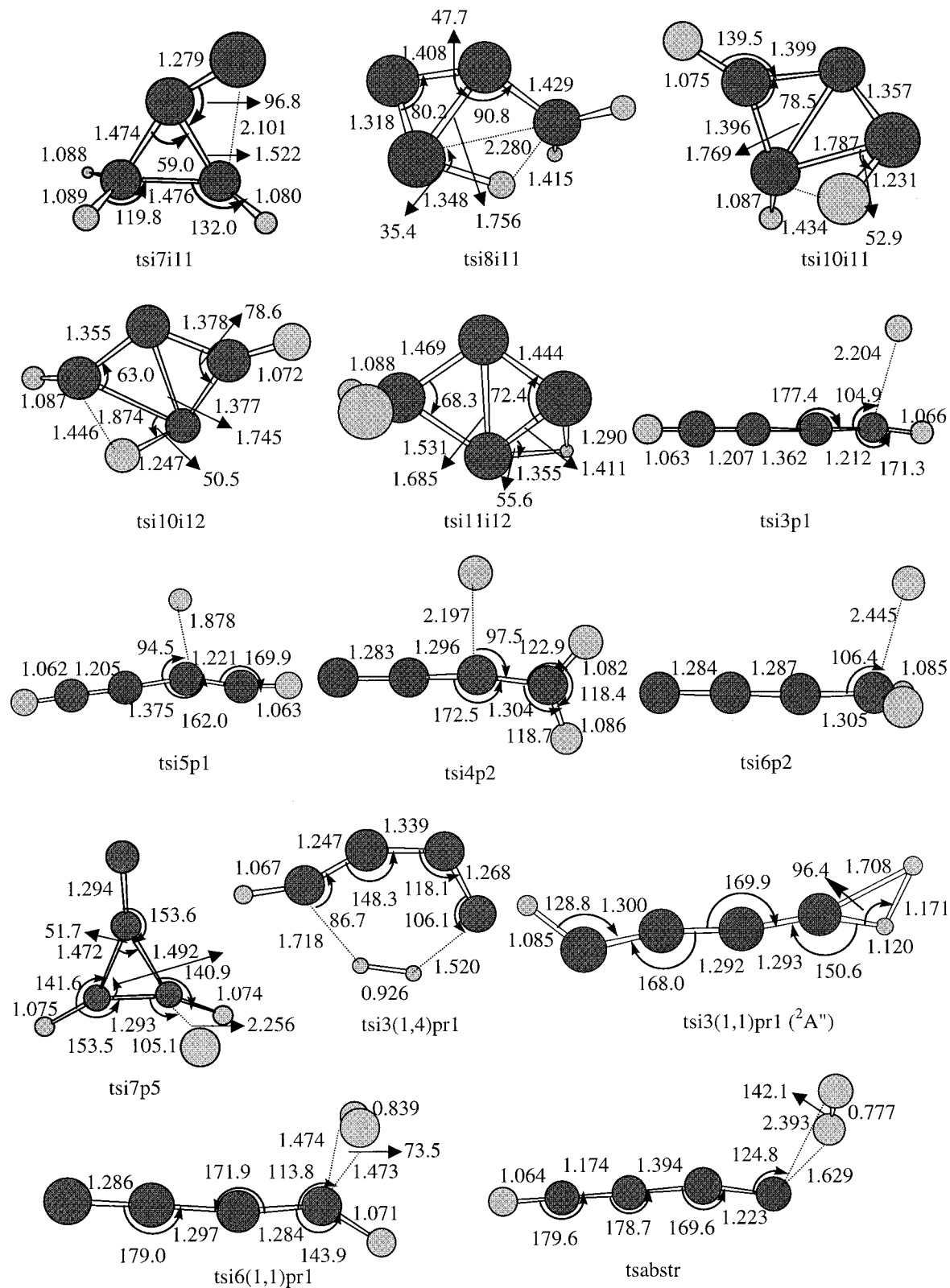| Species	B3LYP 6-311G(d,p)	ZPE (kcal/mol)	MP2 6-311G(d,p)	CCSD(T) 6-311G(d,p)	MP2 6-311+G(3df,2p)	G2M(RCC,MP2)[a] (kcal/mol)
C(^{3}P$_j$) + C$_3$H$_3$(X^{2}B$_1$)	−153.89335	25.69	−153.39197	−153.47114	−153.47315	0.0
i1	−154.06105	29.34	−153.56725	−153.62739	−153.66008	−101.7
i2	−154.02995	27.57	−153.50836	−153.59346	−153.59527	−78.5
i3[b]	−154.11559	28.30	−153.58483	−153.67566	−153.67468	−131.2
i4	−154.05609	30.31	−153.52987	−153.62698	−153.61722	−97.0
i5-cis	−154.09015	29.45	−153.58196	−153.65847	−153.67246	−119.6
i5-trans	−154.09033	29.61	−153.58264	−153.65826	−153.67308	−119.3
i6	−154.05154	29.27	−153.53719	−153.61557	−153.62577	−91.7
i7	−154.02531	29.29	−153.52922	−153.59569	−153.62008	−80.6
i8	−154.05164	29.77	−153.56576	−153.62110	−153.65714	−96.4
i9	−154.05783	29.14	−153.56262	−153.62311	−153.65588	−99.5
i10	−154.02988	29.51	−153.51638	−153.60333	−153.60549	−84.1
i11	−154.02493	30.50	−153.53884	−153.59982	−153.62991	−82.1
i12	−154.05430	31.07	−153.57277	−153.63079	−153.66349	−100.8
p1 + H	−154.03059	23.53	−153.55850	−153.60176	−153.64959	−90.3
p2 + H	−154.96387	22.29	−153.47250	−153.53094	−153.56285	−46.7
p3 + H		28.00[c]	−153.39644	−153.44520	−153.48723	12.6
p4 + H	−153.92508	23.65	−153.46514	−153.51068	−153.55490	−32.2
p5 + H	−153.91508	22.35	−153.43089	−153.48956	−153.52231	−21.3
pr1	−153.98087	24.67	−153.45567	−153.55175	−153.54332	−55.7
tsi1i2		29.54[c]	−153.50930	−153.58217	−153.59876	−71.0
tsi1i3	−154.02530	28.08	−153.51619	−153.59214	−153.60842	−80.5
tsi1i11	−154.00589	28.77	−153.51097	−153.57676	−153.60298	−70.0
tsi1i12	−154.02694	29.35	−153.51880	−153.59660	−153.61060	−81.7
tsi2i3	−154.02972	26.80	−153.50957	−153.59304	−153.59970	−81.0
tsi2i4	−153.99156	25.39	−153.46833	−153.54895	−153.56082	−56.2
tsi2i5	−153.96817	25.57	−153.43216	−153.53641	−153.52020	−45.4
tsi3i4	−153.97130	26.64	−153.45652	−153.53893	−153.54865	−48.5
tsi3i5	−154.02046	25.13	−153.50992	−153.58104	−153.60456	−78.0
tsi3i6	−153.95491	26.37	−153.45770	−153.52695	−153.54733	−39.6
tsi4i6	−153.98997	27.05	−153.48011	−153.54770	−153.57279	−53.9
tsi4i7	−154.01760	29.03	−153.50451	−153.58230	−153.59509	−72.3
tsi5i9	−154.04712	27.72	−153.54265	−153.61163	−153.63555	−93.5
tsi5i10	−154.00905	28.54	−153.47394	−153.57809	−153.56268	−69.0
tsi6i8	−154.00417	28.52	−153.50575	−153.57483	−153.59478	−67.2
tsi7i11	−154.01142	29.55	−153.52275	−153.58454	−153.61312	−73.1
tsi8i11		29.93[c]	−153.46330	−153.52558	−153.55334	−35.5
tsi10i11	−153.96100	26.68	−153.46391	−153.53435	−153.55454	−44.6
tsi10i12	−153.96861	26.51	−153.48241	−153.53983	−153.57431	−49.0
tsi11i12	−153.94472	26.61	−153.45229	−153.52184	−153.54324	−37.0
tsi3p1	−154.02971	23.84	−153.54151	−153.59688	−153.62650	−83.1
tsi5p1	−154.02263	24.05	−153.50263	−153.58759	−153.59428	−81.3
tsi4p2	−153.96120	23.14	−153.45627	−153.52452	−153.54710	−42.1
tsi6p2	−153.96384	27.88	−153.43548	−153.51973	−153.52590	−34.1

the CH bond strength in **i3** as 40.9 kcal/mol. The reverse reaction **p1** + H on the doublet PES was found to have barriers of 7.2 kcal/mol to produce **i3** and 9.0 kcal/mol to form **i5**. Thus, the barriers for H addition to diacetylene are higher than that for H addition to acetylene: 5.8 kcal/mol at the CCSD(T)/6-311 + G(3df,2p)//B3LYP/6-311G(d,p) level.[44]

The next stable isomer, butatrienylidene (**p2**), has C_{2v} symmetry and the $^1A_1$ electronic state and lies 43.6 kcal/mol higher in energy than diacety-

TABLE I.
(Continued)

Species	B3LYP 6-311G(d,p)	ZPE (kcal/mol)	MP2 6-311G(d,p)	CCSD(T) 6-311G(d,p)	MP2 6-311+G(3df,2p)	G2M(RCC,MP2)[a] (kcal/mol)
tsi7p5	−153.91388	22.88	−153.42123	−153.48513	−153.51381	−18.7
tsabstr		25.89[c]	−153.46100	−153.54231	−153.55269	−51.1
tsi3(1,4)**pr1**	−153.93385	23.29	−153.42693	−153.49964	−153.51835	−26.7
tsi6(1,1)**pr1**	−153.95141	23.10	−153.43250	−153.50230	−153.52528	−29.4
n-C_4H_3($^2A''$)		29.60[c]	−153.52620	−153.59732	−153.61840	−83.6
tsi3(1,1)**pr1**($^2A''$)		24.00[c]	−153.37938	−153.45525	−153.47246	−0.4
$C_2H + HCCH$	−153.98416	25.80	−153.48807	−153.56292	−153.57507	−61.1
$C_2H + H_2CC$	−153.91475	23.72	−153.40591	−153.49297	−153.49180	−18.8

[a] Relative energies.

[b] CCSD(T)/6-311G(d,p) optimized geometry (**i3b**) was used for single-point energy calculations at the G2M(RCC,MP2) level, but the ZPE was taken from B3LYP/6-311G(d,p) calculations for **i3a**.

[c] Geometry and frequencies were calculated at the MP2/6-311G(d,p) level.

lene (**p1**). Isomer **p2** can be obtained by hydrogen elimination from **i4** and **i6** through product-like transition states located 4.6 and 12.6 kcal/mol, respectively, above the product, as well as from **i3** without an exit barrier. Another isomer is singlet **p4** with a four-member ring that is 58.1 kcal/mol above **p1**, which belongs to the C_s point group and has a $^1A'$ electronic wave function. Isomer **p4** can be formed by barrierless hydrogen loss in **i11** and **i12**.

A less stable C_4H_2 isomer, cyclopropenyl-idenecarbene (**p5**) has C_{2v} symmetry and the $^1A_1$ electronic state, lies 69.0 kcal/mol higher than **p1**, and can be formed by a H-atom loss from either **i7** with an exit barrier of 2.6 kcal/mol or **i9** without an exit barrier. We surveyed the least stable isomer **p3**, which also has a four-member ring structure with C_{2v} symmetry and an $^1A_1$ electronic state. According

to our calculations, **p3** lies 102.9 kcal/mol above **p1** and can be produced by barrierless hydrogen loss from **i10** and **i11**.

In addition, we considered other dissociation channels leading to the $HCCCC(C_{\infty v}, {}^2\Sigma^+) + H_2$ (**pr1**) fragmentation products. The product **pr1** lies 34.6 kcal/mol above **p1** and is formed by molecular hydrogen elimination from **i3** and **i6**. The H_2 elimination from **i3** occurs via transition state tsi3(1,4)pr1 and involves one hydrogen atom from the CH_2 group and another one from the CH fragment. Isomer **i6** undergoes a 1,1-H_2 elimination via tsi6(1,1)pr1. In both cases the corresponding barriers are high and the transition states tsi3(1,4)pr1 and tsi6(1,1)pr1 lie 29.0 and 26.3 kcal/mol, respectively, above the product. Despite a careful search, we were not able to find a transition state for a 1,1-H_2 elimination from **i3**. The saddle point optimization always converges to tsabstr (C_s, $^2A'$), which actually connects the C_4H_2 (**p1**) + H and $HCCCC(^2\Sigma^+) + H_2$ products, according to the IRC calculations. The energy of this transition state is rather low at only 4.6 kcal/mol above **pr1** and 51.1 kcal/mol below the $C(^3P_j) + C_3H_3(^2B_1)$. However, under single collision

TABLE II.
RRKM Rate Constants (s^{-1}) at Internal Energies of 0.0 and 10.0 kcal/mol above Reactant Zero-Point Level.

		0.0 kcal/mol	10.0 kcal/mol
k_1	(**i1** → **i3**)	3.03×10^{12}	3.78×10^{12}
k_2	(**i1** → **i12**)	4.48×10^{11}	3.70×10^{11}
k_3	(**i1** → **i11**)	8.85×10^{10}	1.25×10^{11}
k_4	(**i3** → **p1**)	6.61×10^{13}	8.35×10^{13}
k_5	(**i3** → **i5**)	7.27×10^{12}	1.14×10^{13}
k_{-5}	(**i5** → **i3**)	2.01×10^{12}	3.02×10^{12}
k_6	(**i3** → **i6**)	1.49×10^{8}	5.05×10^{8}
k_7	(**i3** → **i4**)	1.42×10^{9}	3.71×10^{9}
k_8	(**i5** → **p1**)	3.18×10^{10}	4.65×10^{12}

TABLE III.
Product Yield (%) at Internal Energies of 0.0 and 10.0 kcal/mol above Reactant Zero-Point Level.

	0.0 kcal/mol	10.0 kcal/mol
HCCCCH (from **i5**)	6.7	8.3
HCCCCH (from **i3**)	93.3	91.7
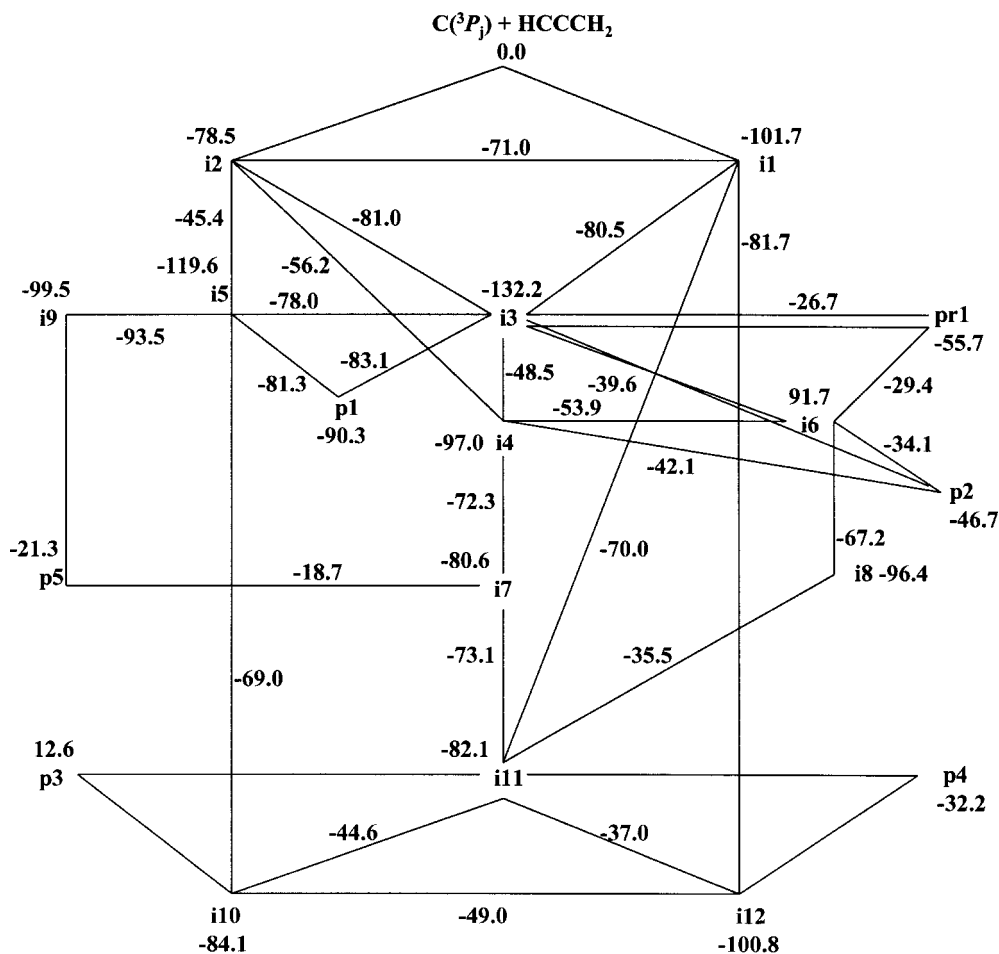
FIGURE 3. A graph of possible isomerization and dissociation pathways on the potential energy surface of the C$_4$H$_3$ radical. The relative energies (kcal/mol) are calculated at the G2M(RCC,MP2) level.

conditions in crossed molecular beam experiments the C$_4$H$_2$ + H reaction cannot occur. Interestingly, the secondary HCCCC($^2\Sigma^+$) + H$_2$ reaction is not likely to proceed by the molecular hydrogen addition pathway because the barriers for the 1,1-H$_2$ addition to the CH group and the 1,4-H$_2$ addition are high (26–29 kcal/mol) and no first-order saddle point exists for the 1,1-H$_2$ addition to the terminal carbon. Instead, the reaction is expected to go by the abstraction mechanism leading to C$_4$H$_2$ + H through a low barrier. It is noteworthy that a similar reaction HCC($^2\Sigma^+$) + H$_2$ exclusively produces C$_2$H$_2$ + H by hydrogen abstraction with a barrier of 2–3 kcal/mol.[45]

A minor amount of the H$_2$ product was observed in recent crossed molecular beam experiments measuring the C$_2$D + C$_2$H$_2$ reaction.[46] Neither 1,4-H$_2$ elimination from **i3** nor 1,1-H$_2$ elimination from **i6** can account for this loss. To explore the possibility of the H$_2$ formation from C$_4$H$_2$D, we investigated this

channel for the excited ^{2}A″ surface of C$_4$H$_3$. The first excited state of the product, HCCCC($^2\Pi$), lies only ~72 cm^{-1} higher in energy than HCCCC($^2\Sigma^+$),[47] and the ^{2}A″ PES correlates to HCCCC($^2\Pi$) + H$_2$. We optimized the structure of n-C$_4$H$_3$ in the ^{2}A″ electronic state (see Fig. 1). The calculations showed that n-C$_4$H$_3$(^{2}A″) lies 83.6 kcal/mol below C(^3P_j) + C$_3$H$_3$(^{2}B$_1$) at the G2M(RCC,MP2) level, which is about 48 kcal/mol above the ground state n-C$_4$H$_3$(^{2}A′) **i3**. The n-C$_4$H$_3$(^{2}A″) can dissociate and produce HCCCC($^2\Pi$)+H$_2$ via tsi3(1,1)pr1 (^{2}A″), but the barrier is high at 83.2 kcal/mol. The transition state lies only 0.4 kcal/mol below the reactants. The IRC calculations confirmed that tsi3(1,1)pr1 (^{2}A″) connects n-C$_4$H$_3$(^{2}A″) and the HCCCC($^2\Pi$) + H$_2$ products. This channel opens a possibility of H$_2$ formation in the C$_2$D + C$_2$H$_2$ reaction, but the excited state PES has to be involved. Taking into account that the first excited state of diacetylene (^{3}B$_u$) lies about 4 eV (92 kcal/mol) higher in energy than the

FIGURE 4. Potential energy profiles of the most important pathways for the C(^3P_j) + HCCCH$_2$(X^{2}B$_1$) reaction. The relative energies (kcal/mol) are calculated at the G2M(RCC,MP2) level.

ground state,[48] the HCCCC($^2\Pi$) + H$_2$ product channel on the excited state PES can compete with the atomic hydrogen elimination, HCCCCH(^{3}B$_u$) + H. Further careful studies of the ^{2}A″ PES for C$_4$H$_3$ and its crossing with the ground ^{2}A′ surface are required in order to clarify the C$_2$D + C$_2$H$_2$ → DCCCC + H$_2$ reaction mechanism.

Other possible products of the C(^3P_j)+C$_3$H$_3$ (^{2}B$_1$) reaction are C$_2$H + H$_2$CC and C$_2$H + HCCH, which can be formed by C—C bond cleavages in **i3** and **i5**, respectively. As seen in Figure 4, both these product channels are exothermic (by 18.8 kcal/mol for C$_2$H+H$_2$CC and 61.1 kcal/mol for C$_2$H+acetylene) and exhibit no exit barriers. Thus, the reverse reactions of the ethynyl radical with vinylidene and acetylene are expected to be fast and to have a negative temperature dependence of their rate constants. This is indeed the case for the C$_2$H + HCCH reaction.[28]

MOST FAVORABLE MECHANISM OF C(^3P_J) + HCCCH$_2$(X^{2}B$_1$) REACTION

According to the schematic PES for C(^3P_j) + HCCCH$_2$(X^{2}B$_1$) (see Fig. 4), the reaction can proceed by two different channels without an entrance barrier. The first is the addition of the carbon atom to the π system at the acetylenic carbon atom of the propargyl radical to produce metastable **i2**, which immediately undergoes a barrierless 1,2-H shift leading to **i3**. The second channel is the addition to the acetylenic C≡C bond yielding **i1**. Both channels produce **i3**; the rate constant k_1 for the **i1** → **i3** isomerization is 6.8 and 34 times higher than k_2 for **i1** → **i12** and k_3 for **i1** → **i11**, respectively. Interestingly, although the barrier for the **i1** → **i12** isomerization is 1.2 kcal/mol lower than that for **i1** → **i3**, the former process has a slower rate than the latter that is due to the much tighter transition state (see corresponding vibrational frequencies in Supplementary Material). The n-C$_4$H$_3$ radical **i3** dissociates to the singlet diacetylene (**p1**) + H with a barrier of 48.1 kcal/mol relative to **i3**; it isomerizes to **i5**, **i4**, or **i6**; or it undergoes the 1,4-H$_2$ elimination to **pr1**. Because of much higher barriers, the last three processes are not expected to compete with the H loss and the 1,2-H migration to **i5**. For instance, for the internal energy of 10.0 kcal/mol above the reactant level, the calculated rate constant k_5 for **i3** → **i5** is 3070 and 22,800 times higher than k_7 for **i3** → **i4** and k_6 for **i3** → **i6**, respectively. Intermediate **i5** in turn can eliminate a hydrogen atom and produce **p1** + H with a barrier of 38.3 kcal/mol or yield C$_2$H + acetylene without an exit barrier with

endothermicity of 58.5 kcal/mol. Other pathways of isomerization of **i5** cannot compete because of very high barriers. Thus, the C(^3P_j) + HCCCH$_2$(X^{2}B$_1$) reaction is expected to almost exclusively produce the singlet diacetylene HCCCCH and a hydrogen atom, while minor contributions from the C$_4$H + H$_2$ and C$_2$H + C$_2$H$_2$ product channels cannot be completely excluded.

Using the rate constants k_4, k_5, k_{-5} (**i5** → **i3**) and k_8 (**i5** → **p1** + H), we solved the kinetic rate equations for the following reaction employing the steady-state approximation[43]:

$$\textbf{i3} \underset{k_{-5}}{\overset{k_5}{\rightleftarrows}} \textbf{i5} \xrightarrow{k_8} \text{HCCCCH} + \text{H}$$
$$\downarrow k_4 \uparrow$$

The results (Table III) show that at an internal energy of 10.0 kcal/mol above the reactant level the **p1** + H products are produced mostly from the n-C$_4$H$_3$ isomer **i3** (91.7%) and, in part, from i−C$_4$H$_3$ **i5** (8.3%).

COMPARISON TO CROSSED BEAM REACTION OF C(^3P_J) WITH HCCCH$_2$

Recently, the reaction of the C(^3P_j) with a propargyl radical (HCCCH$_2$) was investigated at an average collision energy of 10.0 kcal/mol employing the crossed molecular beams technique and a universal mass spectrometric detector.[27] The reaction dynamics were found to be indirect via an osculating complex and governed by an initial attack of C(^3P_j) to the π-electron density of the propargyl radical without an entrance barrier, followed by a 1,2-hydrogen migration to the n-C$_4$H$_3$ isomer. A final C—H bond rupture yielded atomic hydrogen and diacetylene through an exit transition state located 7.2–14.3 kcal/mol above the products.

The experimental and theoretical approaches are highly complementary because the crossed beam experiments could not identify the minor contribution from a decomposing i-C$_4$H$_3$ intermediate **i5**, as well as formation of HCCCC($^2\Sigma^+$) or C$_2$H + C$_2$H$_2$. Both these studies confirmed that the reaction of C(^3P_j) with C$_3$H$_3$ provides an alternative pathway to diacetylene that was hitherto thought to be solely synthesized via reaction (1).[26]

Conclusions

The reaction between a ground-state carbon atom, C(^3P_j), and a propargyl radical, HCCCH$_2$

(X^2B_1), was studied by using the G2M(RCC,MP2) method. The PES, the structures for the stationary points and transition states, as well as the dissociation pathways of various doublet C_4H_3 isomers leading to distinct C_4H_2 structures and atomic hydrogen were investigated. We concluded that at the initial step of the $C(^3P_j) + HCCCH_2(X^2B_1)$ reaction the carbon atom attacked the π system of the acetylenic carbon atom of the propargyl radical and "inserted" into the acetylenic C—H bond or added to the triple C≡C bond without entrance barriers. n-C_4H_3 (i3) was identified as the decomposing complex that formed diacetylene and a hydrogen atom. In a minor amount, i3 underwent a 1,2-H migration prior to an H atom emission and formed diacetylene. Diacetylene was concluded to be a nearly exclusive product of the $C(^3P_j) + HCCCH_2(X^2B_1)$ reaction with a possible minor contribution of the $HCCCCC + H_2$ and $C_2H + HCCH$ products.

Acknowledgments

References

1. Herbst, E.; Lee, H. H.; Howe, D. A.; Millar, T. J. Mon Not R Astron Soc 1994, 268, 335.

2. (a) Kaiser, R. I.; Ochsenfeld, C.; Head-Gordon, M.; Lee, Y. T.; Suits, A. G. Science 1996, 274, 1508; (b) Ochsenfeld, C.; Kaiser, R. I.; Suits, A. G.; Lee, Y. T.; Head-Gordon, M. J Chem Phys 1997, 106, 4141.

3. Almond, M. J., Ed. Short-Lived Molecules; Ellis Horwood: New York, 1990.

4. Foord, J. S.; Loh, K. P.; Singh, N. K.; Jackman, R. B.; Davies, G. J. J Cryst Growth 1996, 164, 208.

5. Gautier, D.; Owen, T. in Origin and Evolution of Planetary and Satellite Atmospheres; Atreya, S. K.; Pollack, J. B.; Matthews, M. S., Eds.; University of Arizona: Tucson, AZ, 1989; p. 487.

6. (a) Yung, Y. L.; Allen, M.; Pinto, J. P. Astrophys J Suppl Ser 1984, 55, 465; (b) Yung, Y. L. Icarus 1987, 72, 468.

7. Coustenis, A.; Bezard, B.; Gautier, D.; Samuelson, R. Icarus 1991, 89, 152.

8. (a) Romani, P. N.; Atreya, S. K. Icarus 1988, 74, 424; (b) Romani, P. N.; Atreya, S. K. Geophys Res Lett 1989, 16, 941.

9. (a) Atreya, S. K.; Sandel, B. R.; Romani, P. N. In Uranus; Bergstralh, J. T., Ed.; University of Arizona: Tucson, AZ, 1990; (b) Summers, M. E.; Strobel, D. F. Astrophys J 1989, 346, 495.

10. Pollack, J. B.; Rages, K.; Pope, S. K.; Tomasko, M. G.; Romani, P. N.; Atreya, S. K. J Geophys Res 1987, 92, 15037.

11. Thompson, W. R.; Singh, S. K.; Khare, B. N.; Sagan, C. Geophys Res Lett 1989, 16, 981.

12. West, R. A.; Strobel, D. F.; Tomasko, M. G. Geophys Res Lett 1986, 65, 161.

13. (a) Karkoschka, E.; Tomasko, M. G. Icarus 1992, 97, 161; (b) Chen, F.; Judge, D. L.; Wu, C. Y. R.; Caldwell, J.; White, H. P.; Wagener, R. J Geophys Res 1991, 96, 17519.

14. Kunde, V. G.; Aikin, A. C.; Hanel, R. A.; Jennings, D. E.; Maguire, W. C.; Samuelson, R. E. Nature 1981, 292, 686.

15. Hardwick, J. L.; Ramsay, D. A. Chem Phys Lett 1977, 48, 399.

16. Haink, H.-J.; Jungen, M. Chem Phys Lett 1979, 61, 319.

17. Lamotte, J.; Binet, C.; Romanet, R. J Chim Phys 1977, 74, 577.

18. Price, W. C.; Walsh, A. D. Trans Faraday Soc 1945, 41, 381.

19. Smith, W. L. Proc R Soc London Ser A 1967, 300, 519.

20. Koster-Jensen, E.; Haink, H.-J.; Christen, H. Helv Chim Acta 1974, 57, 1731.

21. Allan, M. J Chem Phys 1984, 80, 6020.

22. (a) Bandy, R. E.; Lakshminarayan, C.; Frost, R. K.; Zwier, T. S. Science 1992, 258, 1630; (b) Bandy, R. E.; Lakshminarayan, C.; Frost, R. K.; Zwier, T. S. J Chem Phys 1993, 98, 5362.

23. Harris, S. J.; Wiener, A. M. Annu Rev Phys Chem 1985, 36, 31.

24. Hou, K. C.; Anderson, R. C. J Phys Chem 1963, 67, 1579.

25. Seki, K.; Nakashima, N.; Nishi, N.; Kinoshita, M. J Chem Phys 1986, 85, 274.

26. Pedersen, J. O. P.; Opansky, B. J.; Leone, S. R. J Phys Chem 1993, 97, 6822.

27. Kaiser, R. I.; Sun, W.; Suits, A. G.; Lee, Y. T. J Chem Phys 1997, 107, 8713.

28. Chastaing, D.; James, P. L.; Sims, I. R.; Smith, I. W. M. Faraday Disc 1998, 109, 165.

29. (a) Le, T. N.; Lee, H.-Y.; Mebel, A. M.; Kaiser, R. I. J Phys Chem A 2001, 105, 1847; (b) Kaiser, R. I.; Lee, Y. T.; Suits, A. G. J Chem Phys 1996, 105, 8705.

30. Nguyen, T. L.; Mebel, A. M.; Kaiser, R. I. J Phys Chem A 2001, 105, 3289.

31. (a) Mebel, A. M.; Kaiser, R. I.; Lee, Y. T. J Am Chem Soc 2000, 122, 1776; (b) Kaiser, R. I.; Mebel, A. M.; Chang, A. H. H.; Lin, S. H.; Lee, Y. T. J Chem Phys 1999, 110, 10330; (c) Kaiser, R. I.; Stranges, D.; Lee, Y. T.; Suits, A. G. J Chem Phys 1996, 105, 8721.

32. (a) Kaiser, R. I.; Hahndorf, I.; Huang, L. C. L.; Lee, Y. T.; Bettinger, H. F.; Schleyer, P. v. R.; Schaefer, III, H. F.; Schreiner, P. R. J Chem Phys 1999, 110, 6091; (b) Bettinger, H. F.; Schleyer, P. v. R.; Schaefer, H. F.; Schreiner, P. R.; Kaiser, R. I.; Lee, Y. T. J Chem Phys 2000, 113, 4250; (c) Kaiser, R. I.; Asvany, O.; Lee, Y. T. Planet Space Sci 2000, 48, 483; (d) Handorf, I.; Lee, H. Y.; Mebel, A. M.; Lin, S. H.; Lee, Y. T.; Kaiser, R. I. J Chem Phys 2000, 113, 9622; (e) Huang, L. C. L.; Lee, H. Y.; Mebel, A. M.; Lin, S. H.; Lee, Y. T.; Kaiser, R. I. J Chem Phys 2000, 113, 9637.

33. Ha, T. K.; Gey, E. J Mol Struct (THEOCHEM) 1994, 112, 197.

34. (a) Becke, A. D. J Chem Phys 1993, 98, 5648; (b) ibid 1992, 96, 2155; (c) ibid 1992, 97, 9173; (d) Lee, C.; Yang, W.; Parr, R. G. Phys Rev 1988, B37, 785.

35. Krishnan, R.; Frisch, M.; Pople, J. A. J Chem Phys 1980, 72, 4244.

36. Hehre, W. J.; Radom, L.; Schleyer, P.; Pople, J. Ab Initio Molecular Orbital Theory Wiley: New York, 1996.

37. (a) Purvis, G. D.; Bartlett, R. J. J Chem Phys 1982, 76, 1910; (b) Hampel, C.; Peterson, K. A.; Werner, H.-J. Chem Phys

Lett 1992, 190, 1; (c) Knowles, P. J.; Hampel, C.; Werner, H.-J. J Chem Phys 1994, 99, 5219; (d) Deegan, M. J. O.; Knowles, P. J. Chem Phys Lett 1994, 227, 321.

38. Mebel, A. M.; Morokuma, K.; Lin, M. C. J Chem Phys 1995, 103, 7414.

39. (a) Curtiss, L. A.; Raghavachari, K.; Trucks, G. W.; Pople, J. A. J Chem Phys 1991, 94, 7221; (b) Pople, J. A.; Head-Gordon, M.; Fox, D. J.; Raghavachari, K.; Curtiss, L. A. J Chem Phys 1989, 90, 5622; (c) Curtiss, L. A.; Jones, C.; Trucks, G. W.; Raghavachari, K.; Pople, J. A. J Chem Phys 1990, 93, 2537;

40. (a) Curtiss, L. A.; Raghavachari, K.; Pople, J. A. J Chem Phys 1993, 98, 1293; (b) Smith, B. J.; Radom, L. J Phys Chem 1995, 99, 6468; (c) Curtiss, L. A.; Redfern, P. C.; Smith, B. J.; Radom, L. J Chem Phys 1996, 104, 5148.

41. (a) Curtiss, L. A.; Raghavachari, K.; Redfern, P. C.; Pople, J. A. J Chem Phys 1997, 106, 1063; (b) Curtiss, L. A.; Redfern, P. C.; Raghavachari, K.; Pople, J. A. J Chem Phys 1998, 109, 42.

42. Frisch, M. J.; Trucks, G. W.; Schlegel, H. B.; Scuseria, G. E.; Robb, M. A.; Cheeseman, J. R.; Zakrzewski, V. G.; Montgomery, J. A.; Stratmann, R. E.; Burant, J. C.; Dapprich, S.; Millam, J. M.; Daniels, A. D.; Kudin, K. N.; Strain, M. C.; Farkas, O.; Tomasi, J.; Barone, V.; Cossi, M.; Cammi, R.; Mennucci, B.; Pomelli, C.; Adamo, C.; Clifford, S.; Ochterski, J.; Petersson, G. A.; Ayala, P. Y.; Cui, Q.; Morokuma, K.; Malick, D. K.; Rabuck, A. D.; Raghavachari, K.; Foresman, J. B.; Cioslowski, J.; Ortiz, J. V.; Stefanov, B. B.; Liu, G.; Liashenko, A.; Piskorz, P.; Komaromi, I.; Gomperts, R.; Martin, R. L.; Fox, D. J.; Keith, T.; Al-Laham, M. A.; Peng, C. Y.; Nanayakkara, A.; Gonzalez, C.; Challacombe, M.; Gill, P. M. W.; Johnson, B.; Chen, W.; Wong, M. W.; Andres, J. L.; Head-Gordon, M.; Replogle, E. S.; Pople, J. A. Gaussian 98, Revision A.5; Gaussian, Inc.: Pittsburgh, PA, 1998.

43. Eyring, H.; Lin, S. H.; Lin, S. M. Basic Chemical Kinetics; Wiley: New York, 1980.

44. Chang, A. H. H.; Mebel, A. M.; Yang, X.-M.; Lin, S. H.; Lee, Y. T. J Chem Phys 1998, 109, 2748.

45. Kurosaki, Y.; Takanayanagi, T. J Chem Phys 2000, 113, 4060.

46. Kaiser, R. I.; et al. unpublished.

47. (a) Woon, D. E. Chem Phys Lett 1995, 244, 45; (b) Sobolewski, A. L.; Adamovicz, L. J Chem Phys 1994, 102, 394; (c) Kolbuszewski, M. Astrophys J 1994, 432, L63.

48. Karpfen, A.; Lischka, H. Chem Phys 1986, 102, 91.